

Ozone Depletion from Nearby Supernovae

Neil Gehrels

e-mail: gehrels@lheapop.gsfc.nasa.gov

NASA/GSFC/Laboratory for High Energy Astrophysics, Code 661, Greenbelt, MD 20771

Claude M. Laird

e-mail: claird@ku.edu

Department of Physics and Astronomy, University of Kansas, Lawrence, KS 66045

Charles H. Jackman

e-mail: jackman@assess.gsfc.nasa.gov

NASA/GSFC/Laboratory for Atmospheres, Code 916, Greenbelt, MD 20771

John K. Cannizzo¹

e-mail: cannizzo@stars.gsfc.nasa.gov

NASA/GSFC/Laboratory for High Energy Astrophysics, Code 661, Greenbelt, MD 20771

Barbara J. Mattson²

e-mail: mattson@milkyway.gsfc.nasa.gov

NASA/GSFC/Laboratory for High Energy Astrophysics, Code 661, Greenbelt, MD 20771

Wan Chen

e-mail: Wan.W.Chen@mail.sprint.com

Sprint, IP Design – RAD, 12502 Sunrise Valley Dr., Reston, VA 20196

to appear in the *Astrophysical Journal* 2003, March 10, vol. 585

Received 2002 May 28; accepted 2002 November 12

¹also University of Maryland Baltimore County

²also L3 Com Analytics Corp.

ABSTRACT

Estimates made in the 1970’s indicated that a supernova occurring within tens of parsecs of Earth could have significant effects on the ozone layer. Since that time improved tools for detailed modeling of atmospheric chemistry have been developed to calculate ozone depletion, and advances have been made also in theoretical modeling of supernovae and of the resultant gamma-ray spectra. In addition, one now has better knowledge of the occurrence rate of supernovae in the galaxy, and of the spatial distribution of progenitors to core-collapse supernovae. We report here the results of two-dimensional atmospheric model calculations that take as input the spectral energy distribution of a supernova, adopting various distances from Earth and various latitude impact angles. In separate simulations we calculate the ozone depletion due to both gamma-rays and cosmic rays. We find that for the combined ozone depletion from these effects roughly to double the “biologically active” UV flux received at the surface of the Earth, the supernova must occur at $\lesssim 8$ pc. Based on the latest data, the time-averaged galactic rate of core-collapse supernovae occurring within 8 pc is $\sim 1.5 \text{ Gyr}^{-1}$. In comparing our calculated ozone depletions with those of previous studies, we find them to be significantly less severe than found by Ruderman (1974), and consistent with Whitten et al. (1976). In summary, given the amplitude of the effect, the rate of nearby supernovae, and the ~ 0.5 Gyr time scale for multicellular organisms on Earth, this particular pathway for mass extinctions may be less important than previously thought.

Subject headings: molecular processes; Earth; stars: supernovae: general; supernovae: SN1978A; ISM: cosmic rays

1. Introduction

Ruderman (1974) suggested and was the first to study the reduction of stratospheric O_3 due to enhanced levels of nitrogen oxides caused by incident radiation from a supernova (SN). With rough calculations he found that a nearby (< 17 pc) SN would cause a reduction of O_3 by $\sim 80\%$ for > 2 yr from the gamma radiation, and a 40 – 90% reduction in O_3 lasting hundreds of years from cosmic rays (Ruderman 1974, Laster 1968). Reid et al. (1978) reached similar conclusions, while Whitten et al. (1976) found a much smaller effect. Ellis & Schramm (1995) present a study similar to Ruderman’s in which simple analytical scalings were utilized. Crutzen & Brühl (1996) also examine the problem using a time dependent two-dimensional (2D) model, considering only the enhanced cosmic ray flux. Except for Crutzen & Brühl, these studies used simple theoretical models for the SN energy and had, at best, one-dimensional (1D) photochemistry models. Advances in computing power and atmospheric models now make a more detailed analysis possible. Also, SN1987A observations and recent state-of-the-art calculations provide an estimate for the total gamma-ray input from a core-collapse SN.

2. Methodology

We model the effects of a core-collapse SN on the Earth’s ozone by inputting the expected cosmic and gamma irradiation into an atmospheric model. We consider: (1) the relatively short-lived (~ 100 d) gamma rays from the initial blast, and (2) the longer lived ($\gtrsim 10$ y) cosmic rays accelerated in the SN blast wave. We examine the effects of SN distance and impact angle latitude, and determine the ozone depletion averaged latitudinally and globally.

2.1. Atmospheric Model

We use the NASA/Goddard Space Flight Center (GSFC) two-dimensional photochemical transport model, whose two dimensions are latitude and altitude. The latitude range is from the North pole to the South pole and from the ground up to about 116 km. The GSFC model has 18 latitude bands with a latitude grid spacing of 10 degrees. The altitude range includes 58 evenly spaced logarithmic pressure levels (approximately 2 km vertical grid point separation).

This model, including information about the chemistry and computational approach, was originally described in Douglass et al. (1989) and had an altitude range up to 60 km that included the troposphere, stratosphere, and lower mesosphere. The altitude range was extended through the mesosphere with the inclusion of several additional photochemical reactions, which were discussed in Jackman et al. (1990). Heterogeneous processes occurring on the stratospheric sulfate aerosol layer and on polar stratospheric clouds are important in the stratosphere and are included in the manner described in Considine et al. (1994).

The model uses a look-up table for computation of the photolytic source term, which is employed in calculations of photodissociation rates of atmospheric constituents from sunlight (see Jackman et al., 1996). Reaction rates and photolysis cross sections in the model are consistent with the Jet Propulsion Laboratory recommendations (DeMore et al., 1997).

The model includes both winds and small scale mixing processes in the manner described in Fleming et al. (1999), which is briefly reiterated here. The meridional (north-south) and vertical (up-down) winds are climatological in nature. A 17-year average (1979-1995) of temperature data from the National Centers for Environmental Prediction (NCEP) and heating rates from climatological distributions of temperature, ozone, and water vapor are the primary ingredients in deriving the winds. The small scale horizontal

mixing (eddy diffusion) coefficients are obtained self-consistently from the winds and the 17-year NCEP analyses for planetary wave climatology. The small scale vertical mixing (eddy diffusion) coefficients are computed from the mechanical forcing of gravity waves in the mesosphere and upper stratosphere and from the vertical temperature gradient in the troposphere and lower stratosphere.

The model includes a new numerical advection scheme detailed in Fleming et al. (1999), which is mass conserving and utilizes an upstream piecewise parabolic method of solution. A time step of 12 hr is employed for the advection of constituents and a time step of 1 d is used for the computations of changes in the constituents resulting from photochemical reactions.

Recent work with the GSFC 2D model has focused on the influence of solar proton events (SPEs) on atmospheric constituents. Vitt & Jackman (1996) modified the model to incorporate energy deposition by solar protons following Armstrong et al. (1989).

The impact of galactic cosmic rays (GCRs) on the atmosphere was introduced into the model following Nicolet (1975). The Nicolet (1975) study relied on measurements of Neher (1961, 1967, 1971), who made a number of balloon flights which carried instruments to measure ionization rates at various latitudes and pressure. Nicolet used these data to compile the ionization rate (in units of $\text{cm}^{-3} \text{s}^{-1}$) as a function of geomagnetic latitude, altitude, and phase (maximum or minimum) of the solar cycle. These data provide the most reliable estimates of atmospheric ionization rates.

2.2. Inclusion of SN-produced Gamma- and Cosmic Rays

The observed gamma-ray spectrum for SN1987A is

$$\frac{dN}{dE} = 1.7 \times 10^{-3} \left(\frac{E}{1 \text{ MeV}} \right)^{-1.2} \text{ cm}^{-1} \text{ s}^{-1} \text{ MeV}^{-1} \quad (1)$$

(Gehrels et al. 1988) between 0.02 and 2 MeV, lasting 500 d at 55 kpc, for a total energy 9.0×10^{46} erg. For ease of modeling we set the incident monoenergetic gamma-ray photon flux N_i^0 by binning this differential flux into 66 evenly spaced logarithmic intervals from 0.001 to 10 MeV, for a net energy input of 3.3×10^{47} erg. For a given distance D_{SN} we scale the empirically observed SN1987A spectrum by $(5.5 \times 10^4 / D_{\text{SN}})^2$, with D_{SN} in pc. In addition, in our final analysis we rescale our results to a total gamma-ray energy of 1.8×10^{47} erg because of the following: SN1987A was unusual in that its progenitor was a blue supergiant rather than the more typical red supergiant. A recent three-dimensional (3D) smooth particle hydrodynamics (SPH) calculation³ of a SN with a $15M_{\odot}$ red supergiant progenitor gives $\sim [1.8 \pm 0.7] \times 10^{47}$ erg for models which are initially spherically symmetric. In this model, the gamma-ray luminosity peaks at $t \sim 340$ d and is within a factor of 10 of the peak for ~ 500 d. Since the energies of the gamma-ray photons are so much greater than those involved in the atmospheric chemistry reactions, the total input energy is more relevant than the detailed SN spectrum and we therefore have done all scalings using integrated energy inputs.

Treating the energy bins as monoenergetic beams of geometric mean energy $\langle E_i \rangle$ and integrating over a range of energies (from $i = 1$ to 66), the incident photon flux is given

³Aimee Hungerford kindly provided the results of her SN calculations in advance of publication. Her initial model, s15s7b from Weaver & Woosley (1993), was taken 100 s after bounce and mapped into a 3D SPH code. To calculate the gamma-ray spectra and total energies, she mapped time slices from the SN calculation into a 3D Monte Carlo gamma-ray transport code.

by

$$N_i^0 = 8.5 \times 10^{-3} [E_i^{-0.2} - E_{i+1}^{-0.2}] \text{ cm}^{-2} \text{ s}^{-1} \quad (2)$$

where the total incident energy flux in the monoenergetic beam at the top of the atmosphere is $F_i^0 = N_i^0 \langle E_i \rangle$. We attenuate the gamma-ray photon flux with altitude via an exponential decay law, with the frequency-dependent absorption coefficient taken from a look-up table (Plechaty et al. 1981). The beam is propagated vertically through a standard atmosphere, which is adjusted later in the photochemistry model for the appropriate latitude and time of year. The photon flux remaining in a monoenergetic beam is given by $N_{i,j} = N_i^0 e^{-\mu_i x_j}$, where x_j is the column density (in g cm^{-2}) measured from the top of the atmosphere and μ_i is the mass attenuation or absorption coefficient for the i th energy bin (i.e., associated with energy $\langle E_i \rangle$). The photon flux, $\Delta N_{i,j}$ (in photons $\text{cm}^{-2} \text{ s}^{-1}$), deposited in the j th layer with energy $\langle E_i \rangle$, is the difference between $N_{i,j-1}$ and $N_{i,j}$. The energy flux deposited in the j th layer by photons of energy $\langle E_i \rangle$ is $F_{i,j} = \Delta N_{i,j} \langle E_i \rangle$ (in $\text{MeV cm}^{-2} \text{ s}^{-1}$). The total ionization rate is the sum over all energies

$$q_{\text{tot}, j} = \frac{1}{35 \text{ eV}} \sum_{i=1}^{66} \frac{F_{i,j}}{\Delta Z_j}, \quad (3)$$

where 35 eV is the energy required to produce an ion pair (Porter et al. 1976) and ΔZ_j is the thickness of the j th slab.

The energy deposition versus altitude calculated in this way is not dramatically different from that obtained using a detailed radiative transfer model.⁴ Significant energy deposition

⁴We thank David Smith, John Scalo, and Craig Wheeler for kindly sharing results from their Monte Carlo atmospheric radiative transfer calculation. The robustness of adopting simple energy-dependent attenuation coefficients in terms of the energy deposition versus altitude was first shown by Chapman (1931).

into the atmosphere below some altitude $h_{\text{crit}} \sim 16 - 20$ km, depending on latitude, will tend to create ozone rather than to destroy it, therefore one basic check on our assumption of adopting frequency-dependent attenuation coefficients is to compare our fractional energy deposition versus altitude against the radiative transfer calculations of Smith et al. (private communication). We estimate the altitude-dependent energy deposition in our model by taking the Earth’s atmosphere to be exponential $\rho = \rho_0 \exp(-h/H_\rho)$, where the sea level density $\rho_0 = 1.3 \times 10^{-3}$ g cm $^{-3}$ and $H_\rho = 8$ km. (This gives an integrated column density $\Sigma = \rho_0 H_\rho = 1040$ g cm $^{-2}$.) Using the frequency-dependent absorption coefficients from Plechaty et al. (1981) shows that, for photon energies between 0.25 MeV and 2. MeV, for example, the peak energy deposition varies between about 30 and 40 km, well above h_{crit} . The Smith et al. energy deposition at 1 MeV peaks at ~ 32 km. Finally, a detailed comparison of the ratio of fractional energy deposition versus altitude at 1 MeV between our model and Smith et al. shows the ratio to be within ~ 0.2 dex of unity down to $h \simeq 30$ km, and above unity at smaller altitudes where the relative energy deposition drops asymptotically. In the model of Smith et al., the altitude of maximum energy deposition decreases from ~ 34 km to ~ 28 km as the photon energy varies between 0.25 MeV and 2 MeV, while over this same energy range our altitude of maximum energy deposition decreases from ~ 38 km to ~ 30 km. Thus there does not appear to be a significant quantitative difference in the relative energy depositions between the two methods in the region where the dominant deposition occurs – a region which fortuitously lies above h_{crit} in both sets of calculations.

We estimate the SN cosmic ray inputs from the galactic cosmic ray (GCR) ionization rate profiles at various latitudes and solar cycle phase (Vitt & Jackman 1996, Nicolet 1975). The mean rate of nitrogen atom (N) production at different altitudes and latitudes is computed by multiplying the empirically computed rate of ionization (from Nicolet 1975) by 1.25 (Jackman et al. 1990). The N production enhances nitrogen oxide amounts as well

as total odd nitrogen, NO_y (e.g., N , NO , NO_2 , NO_3 , N_2O_5 , HNO_3 , HO_2NO_2 , $ClONO_2$, and $BrONO_2$). The local GCR energy density $\sim 1 \text{ eV cm}^{-3}$ is dominated by protons with a peak at $\sim 0.5 \text{ GeV}$ (Webber 1998), implying a flux $\sim 7 \text{ cm}^{-2} \text{ s}^{-1}$. Each incident cosmic ray produces $\sim 10^7$ ionizing secondary particles. The GCR ionization rate inputs (from Nicolet 1975) were multiplied by 100 to simulate the charged particle flux from a SN at 10 pc, and scaled by $(10 \text{ pc}/D_{\text{SN}})^2$ for other distances. This multiplicative scaling factor was chosen simply and solely to give a total SN energy in cosmic rays consistent with what is currently thought to be a representative value. For $D_{\text{SN}} = 10 \text{ pc}$, the locally observed GCR flux $\sim 0.05 \text{ erg cm}^{-2} \text{ s}^{-1}$ becomes $\sim 5 \text{ erg cm}^{-2} \text{ s}^{-1}$, yielding a total energy $\sim 4 \times 10^{49} \text{ erg}$ over a 20 y run. The corresponding fluence is $\sim 3 \times 10^9 \text{ erg cm}^{-2}$.

The vertical ionization rate profiles are then mapped onto a 2D circular grid, representing a zonally averaged spherical Earth. First a series of ionization rate profiles as functions of atmospheric slab number and latitude are calculated for a flat Earth for incidence angles of 5° , 15° , ..., 85° from the zenith, corresponding to 10° wide latitude bands centered on 85° , 75° , ..., 5° , respectively, for the illuminated hemisphere. These profiles are interpolated to produce vertical average ionization profiles as functions of altitude and latitude. The zenith frame daily ionization profiles are mapped into 360 intervals of 1° longitude and 18 intervals of 10° latitude. Zonally averaged daily ionization rate profiles are produced by averaging over all longitudes for each 10° latitude band, and then input into the GSFC 2D model.

2.3. Atmospheric Model Simulations

Three types of calculations of 20 y duration were carried out: (1) a “base” simulation with no cosmic or gamma rays, (2) “perturbed” simulations with enhanced cosmic ray levels, and (3) “perturbed” simulations with enhanced gamma-rays. The “perturbed”

simulations were compared to the “base” simulation to assess the atmospheric changes. For the cosmic ray trials, the charged particle fluxes are held constant for 20 y, and the results are then checked to ensure a steady state is achieved. For the gamma-ray trials, the irradiation is activated on day 60 (March 1) and maintained at a constant level for 300 d (the SN duration), after which it is attenuated abruptly while the model is run for another 19 y, allowing the perturbed atmosphere time to relax to pre-SN conditions.

3. Results

Atmospheric ozone is easily produced through dissociation of molecular oxygen. The reaction



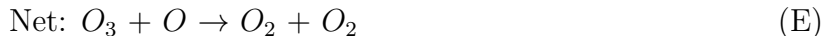
followed by the three-body reaction



illustrates this production process. Reaction (B) as written is schematically representative of the fact that molecular oxygen (O_2) is photodissociated into two atoms of oxygen (O), and each of these attaches with an O_2 to form ozone (O_3), thereby producing two ozone molecules. The M in reaction (B) represents a third body, which is usually either N_2 (78% of the atmosphere) or O_2 (21% of the atmosphere).

Ozone is lost through a number of catalytic reactions involving several “families” or groups of constituents, such as NO_y , HO_x (e.g., H , OH , and HO_2), Cl_y (chlorine-containing inorganic molecules), and Br_y (bromine-containing inorganic molecules). These constituents have both natural and human-made sources, which are explained in several books (e.g., Dessler 2000).

Odd nitrogen, NO_y , is primarily created through natural processes. The major source of NO_y is the oxidation of biologically-produced N_2O in the stratosphere (e.g., Vitt & Jackman 1996). The NO_y constituents can destroy ozone through the catalytic reaction cycle



Note that NO is not consumed through reactions (C) and (D) and the net result is combining an ozone molecule and an atom of oxygen to form two molecules of oxygen. This cycle involving these two reactions can proceed several hundred times before either NO or NO_2 reacts with another atmospheric constituent.

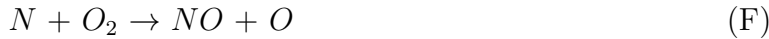
All the “perturbed” simulations include excess NO_y from either cosmic or gamma-rays. We describe the atmospheric effect from these impacts, primarily focusing on the NO_y and O_3 induced variations.

Five gamma-ray simulations were performed for SN impact angle latitude (i.e., latitude for which the SN is at zenith) $i_{\text{SN}} = -90^\circ, -45^\circ, 0^\circ, +45^\circ, \text{ and } +90^\circ$, taking $D_{\text{SN}} = 10$ pc. Three more simulations were carried out for $i_{\text{SN}} = 0^\circ$ and $D_{\text{SN}} = 20, 50, \text{ and } 100$ pc. We find that after 300 d of simulated gamma radiation input, the calculated changes in NO_y and O_3 column density depend significantly on i_{SN} . The largest increases in NO_y for $D_{\text{SN}} = 10$ pc are for $i_{\text{SN}} = \pm 90^\circ$, and exceed 1800% over the poles. The smallest increases occur for $i_{\text{SN}} = 0^\circ$, where the maximum increase is $< 900\%$ by the end of the run. Ozone depletion accompanying the increase in NO_y is greatest for $i_{\text{SN}} = \pm 90^\circ$, with the zone of maximum decrease ($\sim 60\%$) at $60\text{-}70^\circ$ S latitude for $i_{\text{SN}} = -90^\circ$. The smallest decrease occurs for $i_{\text{SN}} = 0^\circ$, with the region of maximum decrease (about 40%) at $60\text{-}90^\circ$ S latitude

(Figures 1 and 2). The maximum annual global average decrease for $D_{\text{SN}} = 10$ pc (Figure 3) is 27% in Year 2 for $i_{\text{SN}} = 0^\circ$; the minimum is 18% for $i_{\text{SN}} = -90^\circ$. Simulations for 10, 20, 50, and 100 pc show a $\sim D_{\text{SN}}^{-n}$ trend in ozone depletion, where $\sim 1.3 < n < \sim 1.9$ (Figure 4). In all cases, the global average ozone depletion from enhanced gamma-rays decreases to a few percent by the sixth or seventh year.

Figure 4 shows an increasing deviation from a D_{SN}^{-2} law for the ozone depletion as D_{SN} decreases. In other words, although the fluence or net energy input from gamma-rays varies (by assumption) as D_{SN}^{-2} , the ozone depletion begins to saturate for small D_{SN} . Three processes lead to this deviation:

1) High production levels of NO_y result in large self-destruction of NO_y and will somewhat limit the modeled concentrations of NO_y (Crutzen & Brühl 1996). The N atoms produced via dissociation of N_2 primarily react to form NO via



however, at higher levels of NO the following reaction is also important



This reaction brings nitrogen out of the odd nitrogen (NO_y) family back to even nitrogen, N_2 .

2) Ozone can be produced (rather than destroyed) by enhancements of NO_y in the troposphere and in the lowest part of the tropical stratosphere (Crutzen & Brühl 1996). The reaction

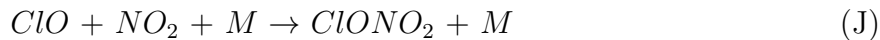


repartitions constituents within the NO_y and HO_x families. NO_2 is rather easily dissociated through



and O_3 is then formed via the three-body reaction (B).

3) Finally, the enhanced NO_y begins to interfere with other families (e.g., chlorine-, bromine-, and hydrogen-containing constituents) that destroy ozone, thus reducing the resultant ozone destruction from those families (e.g., this mechanism for production of NO_y due to extremely large solar proton events was discussed in Jackman et al. 2000). Reactions such as



become important.

For cosmic ray simulations, we find that after achieving the perturbed steady state, NO_y column densities increase at all latitudes and for all times of the year. For $D_{SN} = 10$ pc, the largest increases in column NO_y (650%) occur over the North Pole in late summer, while the smallest increases (200%) occur over the South Pole in winter, with an average global increase of about 350%. Corresponding column O_3 levels decrease globally and in all seasons by as much as 40% over the North Pole, in late summer and by as little as 5% over the equator during May-August for an average global decrease of 22%. Our global ozone reductions are less than those of Ruderman (1974) and Reid et al. (1978), but consistent with Whitten et al. (1976).

4. Uncertainties

The GSFC 2D model has been developed to represent the “present-day” atmosphere. Winds and small-scale mixing processes rely on an average of meteorological field measurements over the 1979-1995 time period and contemporary constituent measurements (see section 2.1). The Earth’s atmosphere has changed dramatically since life first evolved about 3.5 Gyr ago. It has only been since the Cambrian period began (~ 0.55 Gyr ago) that molecular oxygen, and hence ozone, have become significant components of the Earth’s atmosphere. Our computations are, therefore, not applicable to any period before about 0.55 Gyr ago.

If the base state ozone in the past atmosphere, which would have been perturbed by a SN, were radically different from that indicated by recent measured levels of ozone, then the modeled transport field could be fairly different from the actual past atmosphere. Fleming et al. (2001) discussed differences in the total ozone perturbation response from a stratospheric aircraft perturbation. The studied aircraft perturbations were somewhat similar to a SN perturbation since the major atmospheric impact was in the lower stratosphere. Fleming et al. (2001) show about a factor of two variation in the global total ozone perturbation response.

Another possible concern relating to the atmospheric transport is the input energy from cosmic and gamma-rays. This excess energy or “atmospheric heating” can be quantified and compared with background levels of heating: At an altitude of about 15 km or a pressure of about 100 hPa, the background heating rate is $\sim 0.1 - 0.2$ K d⁻¹ (Joan Rosenfield, 1994 personal communication). A heating rate of 0.1 K d⁻¹ corresponds to $\sim 1.9 \times 10^{-3}$ erg cm⁻³ s⁻¹, which is to be compared with the GCR rate of $\sim 1.7 \times 10^{-7}$ erg cm⁻³ s⁻¹. (This assumes an ion pair production of 30 cm⁻³ s⁻¹ at this altitude [from Nicolet 1975] and an energy expended per ion pair of ~ 35 eV [from Porter et al. 1976].) Our *ad hoc* increase by

100 in the GCR rate for $D_{\text{SN}} = 10$ pc raises this volume heating rate to a level that is still only ~ 0.01 of the background rate, which is negligible. A SN would have to be extremely close (i.e., $\lesssim 1$ pc) to drastically perturb the atmosphere through heating.

The focus of this study was on the NO_y production. Both the cosmic and gamma-rays should also produce HO_x (e.g., see Muller & Crutzen 1993). We tried a sensitivity study including the HO_x source in our cosmic ray simulation and assuming 2 HO_x constituents are produced per ion pair. This simulation was only modestly different from the NO_y -only computation and showed reductions of about 1% or so in the calculated total ozone depletion. The reductions in the ozone depletion were caused by interference from the HO_x family constituents with the NO_y family constituents through reactions such as



Other potential uncertainties relating to the atmospheric physics include: 1) input boundary conditions for the source gases, the progenitors of the more reactive atmospheric constituents; 2) reaction rates and photodissociation cross sections; 3) cosmic ray ionization rates from Nicolet (1975) used for scaling the SN input.

The astrophysics portion of the calculation involves additional uncertainties. For instance, the *ad hoc* factor of 100 increase in the GCR rate for $D_{\text{SN}} = 10$ pc was chosen simply so as to produce a CR flux representative of that expected from a SN, and in fact the fluence integrated over 20 yr amounts to $\sim 10^{50}$ erg. (As noted earlier, however, the 20 yr run time in our model was chosen to ensure steady state would be achieved.) Obviously in a more realistic scenario, the increased flux of cosmic rays at the top of the atmosphere would not lead to a uniform elevation of the ionization rate at all altitudes; a proper calculation would involve solving the diffusion of the enhanced flux to lower altitudes. This is beyond our current level of sophistication. In effect, by uniformly augmenting the ionization for all altitudes, we are probably over-representing the increased ionization at the lower

altitudes. Second, for the gamma-ray flux we have also avoided the diffusion (i.e, radiative transfer) problem by adopting simple energy-dependent attenuation coefficients. Although our estimate of the fractional energy deposition versus altitude agrees quantitatively with results from a proper radiative transfer calculation, there may be other intricacies of the process which are not captured in our technique. Finally, there is considerable uncertainty in the duration and functional form (in time) of both the cosmic ray and gamma-ray fluxes. We find that the time to reach steady state in both sets of calculations is relatively short, thus it appears that “flux” is more relevant than “fluence” for our results. Values for the cosmic ray acceleration time Δt_{acc} within the SN remnant ranging from ~ 10 to $\sim 10^5$ yr have been quoted in the literature (Blandford & Eichler 1987, Ellis & Schramm 1995). Our model run time of 20 yr is toward the lower end of this range, therefore if we were to take the additional step of assigning a physical significance to our model run time, our calculated ozone depletion would represent in some sense an upper limit: larger values of Δt_{acc} would dilute the cosmic ray energy in time to a greater extent, and lead to smaller ozone depletions. We feel confident in being able to scale to other values of total adopted energy and “on” time based on the limited number of runs which we calculated. Given the current crude level of understanding of cosmic and gamma-ray fluxes from SNe, it was thought that more complicated assumptions involving additional free parameters, such as power law or exponentially decaying forms for the fluxes, would be unwarranted.

5. Discussion

In order to quantify the impact on life of different levels of ozone depletion, we use the results of Madronich et al. (1998). From their Table 1 and Figure 2, we take a factor of ~ 2 increase in the biologically active UV flux to be a threshold for significant biological effects. This increase corresponds to an ozone depletion of $\sim 47\%$, given that the biologically

active UV flux scales roughly as the reciprocal of the ozone column (Madronich et al. 1998).⁵ There will probably be an interference between the increases in NO_y caused by the gamma-rays and cosmic rays, therefore a summation of the separately computed ozone depletions from the two effects will result in a maximum estimate of the total SN influence. Summing our gamma-ray and cosmic ray depletions for $D_{\text{SN}} = 10$ pc, and taking into account that our adopted energy is larger than that found in the latest SN study mentioned earlier, we obtain a fiducial “critical distance” to significantly disrupt ozone of $D_{\text{crit}} \simeq 8$ pc for a SN with a total gamma-ray energy $\sim 1.8 \times 10^{47}$ erg.

The impulsive addition of energy into the atmosphere by other types of catastrophes may also lead to the production of NO_y , therefore the accompanying destruction of ozone may not be unique to the SN scenario. A geometric dilution factor of $\sim 10^{-22}$ for the cross section of the Earth as seen from 10 pc means that the SN gamma-ray energy of 2×10^{47} erg translates to $\sim 2 \times 10^{25}$ erg intercepted by the Earth. An asteroid with mass $\sim 3 \times 10^{17}$ g and speed ~ 25 km s⁻¹ such as the one responsible for the Cretaceous-Tertiary extinction (Alvarez et al. 1980) has $\sim 10^{30}$ erg of kinetic energy (KE), so that even if as little as $\sim 10^{-5}$ of the KE were channeled into atmospheric heating, it would rival the SN input. On the other hand, the creation of NO_y through a sudden event would probably

⁵Although the exponential, or Beer-Lambert model, for attenuation is a good approximation at a given wavelength, it is not appropriate for biological effects at the Earth’s surface. The biological spectral sensitivity depends on the integrated UV flux between about 290 nm and 330 nm. One can show analytically that the biologically active UV flux varies roughly as the reciprocal of the ozone column given that (i) the ozone absorption cross section decreases exponentially with wavelength in this spectral region (290–330 nm), and (ii) the biological action spectrum decreases exponentially with wavelength over this same spectral region (Madronich et al. 1998).

be less long lasting: First, the transport of NO_y from the stratosphere to the troposphere would occur over a few years. Tropospheric NO_y exists mainly as HNO_3 , and would be removed by precipitation. Second, a localized event in the atmosphere would probably not be communicated globally. For instance, if an asteroid generated NO_y along its trajectory through the atmosphere, it would not necessarily mix globally on a time scale short compared to its destruction time scale. A period of sustained energy input is required to maintain continuously high levels of NO_y if the depletion of ozone is to be effective. On the other hand, the asteroid scenario is known to have many other disastrous effects in terms of atmospheric pollutants. For instance the introduction of massive amounts of sulfur, leading to sulfuric acid, is thought to be devastating to life.

For a nearby SN to disrupt life on Earth, there must be some finite probability that such an event has occurred within the past several hundred million years. For our galaxy the SN rate is ~ 1.5 per century (Cappellaro et al. 1999). Clark et al. (1977) estimate the Sun should pass within 10 pc of a SN during each spiral arm passage, implying a SN rate of $\sim 10 \text{ Gyr}^{-1}$. Two key issues affecting the SN rate are (i) the vertical scale height h_{SN} over which supernovae (SNe) are distributed, and (ii) the displacement of the solar system from the galactic plane. The study of Clark et al., for example, ignores the vertical disk structure and concludes that every passage through a spiral arm results in a close-proximity SN. An opposing view is presented by van den Bergh (1994) who adopts $h_{\text{SN}} = 300 \text{ pc}$, thereby giving $\sim 0.3 \text{ Gyr}^{-1}$ for SNe within 10 pc. Maiz-Apellaniz (2001) utilizes a sample of O-B5 stars, precursors to core-collapse SNe, obtained from the *Hipparchos* catalog to determine $h_{\text{SN}} = 34 \text{ pc}$. He also finds the Sun to be $\sim 24 \text{ pc}$ above the galactic plane – a value that is fortuitously less than h_{SN} . The value $h_{\text{SN}} \simeq 30 \text{ pc}$ is a factor of ~ 10 less than that used by van den Bergh, and leads to a SN rate intermediate between van den Bergh and Clark et al., i.e., $\sim 3 \text{ Gyr}^{-1}$ for $D_{\text{SN}} < 10 \text{ pc}$, or $\sim 1.5 \text{ Gyr}^{-1}$ for $D_{\text{SN}} < D_{\text{crit}} \simeq 8 \text{ pc}$, where we used the fact that the rate varies as D_{SN}^3 .

If the cosmic ray flux scatters off magnetic field irregularities in the interstellar medium, a spread in the arrival times with increasing distance is introduced so that the fluxes vary as D_{SN}^{-4} rather than D_{SN}^{-2} . This comes about because one has a factor D_{SN}^{-2} due to the random walk in spatial spreading, in addition to the normal D_{SN}^{-2} geometric factor (Ellis & Schramm 1995). Benitez et al. (2002) argue that the Earth lies within a bubble of hot gas caused by recent SNe which shields us from the ISM magnetic field, and therefore leads to D_{SN}^{-2} cosmic ray SN fluences. Benitez et al. make this argument concerning recent SNe in the Local Bubble and the Scorpius-Centaurus OB association which may have generated ~ 20 SNe in the last ~ 10 Myr. The cosmic ray flux $\phi_{\text{CR}} \lesssim 1.4 \times 10^7 \text{ erg cm}^{-2} \text{ y}^{-1}$ they quote using the minimal distance for the Sco-Cen SNe $D_{\text{SN}} \gtrsim 40 \text{ pc}$ (and assuming a typical cosmic ray acceleration time $\sim 10 \text{ yr}$) is actually about a factor of 10 less than we adopt in this work for $D_{\text{SN}} = 10 \text{ pc}$, leading us to believe the effect discussed by Benitez et al. may produce ozone depletions of only a few percent. The complications introduced by having the Earth be inside a hot bubble which may enhance the cosmic ray flux during an interval in which several successive SNe occur are interesting and worthy of more detailed studies. It may be the case, for example, that the cumulative effect of having many SNe occur within a relatively short interval is to elevate the general cosmic ray flux within the Local Bubble to a level higher than simple D_{SN}^{-2} fall-off from a single SN would suggest.

6. Conclusion

In summary, we have calculated detailed atmospheric models to determine the extent of the reduction in ozone due to elevated levels of odd nitrogen induced from gamma-rays and cosmic rays produced in a local SN. Our procedure is as follows: (i) We utilize a detailed 2D model for the Earth’s atmosphere, incorporating the latest advances in photochemistry and transport. (ii) For the gamma-ray spectrum we take as input the observed spectrum

from SN1987A, scaling the total energy to the most recent value determined by workers investigating core-collapse SNe with a red supergiant progenitor. (iii) For the cosmic ray spectrum we adopt scaled-up values of the empirically observed ionization rates in the atmosphere from galactic cosmic rays. (iv) To estimate the frequency of local SNe we utilize recent estimates of global SN rates for spiral galaxies and the results of a recent investigation into the vertical spatial extent of core-collapse SN progenitors. Our primary finding is that a core-collapse SN would need to be situated approximately 8 pc away to produce a combined ozone depletion from both gamma-rays and cosmic rays of $\sim 47\%$, which would roughly double the globally-averaged, biologically active UV reaching the ground. The rate of core-collapse SNe occurring within 8 pc is $\sim 1.5 \text{ Gyr}^{-1}$. As noted earlier, our calculated ozone depletion is significantly less than that found by Ruderman (1974), and consistent with Whitten et al. (1976). Given the $\sim 0.5 \text{ Gyr}$ time scale for multicellular life on Earth, this extinction mechanism appears to be less important than previously thought.

It is a pleasure to acknowledge stimulating conversations with Frank Asaro, Narciso Benitez, Adam Burrows, Enrico Cappellaro, Aimee Hungerford, Sasha Madronich, Frank McDonald, Joan Rosenfield, John Scalo, David Smith, Floyd Stecker, Sidney van den Bergh, William Webber, Craig Wheeler, and Stan Woosley.

REFERENCES

- Alvarez, L. W., Alvarez, W., Asaro, F., & Michel, H. V. 1980, *Science*, 208, 1095
- Armstrong, T. P., Laird, C. M., Venkatesan, D., Krishnaswamy, S., & Rosenberg, T. J. 1989, *J. Geophys. Res.*, 94, 3543
- Benitez, N., Maiz-Apellaniz, J., & Canelles, M. 2002, *Phys. Rev. Lett.*, 88, 081101-1
- Blandford, R., & Eichler, D. 1987, *Phys. Rep.*, 154, 1
- Cappellaro, E., Evans, R., & Turatto, M. 1999, *A&A*, 351, 459
- Chapman, S. 1931, *Proc. Phys. Soc.*, 43, 26
- Clark, D. H., McCrea, W. H., Stephenson, F. R. 1977, *Nature*, 265, 318
- Considine, D. B., Douglass, A. R., & Jackman, C. H. 1994, *J. Geophys. Res.*, 99, 18879
- Crutzen, P. J., & Brühl, C. 1996, *Proc. Natl. Acad. Sci. USA*, 93, 1582
- DeMore, W. B., Sander, S. P., Golden, D. M., Hampson, R. F., Kurylo, M. J., Howard, C. J., Ravishankara, A. R., Kolb, C. E., & Molina, M. J. 1997, *Chemical Kinetics and Photochemical Data for Use in Stratospheric Modeling, Evaluation Number 12*, JPL Publication 97-4 (NASA Jet Propulsion Laboratory; Pasadena, California)
- Dessler, A. E. 2000, *The Chemistry and Physics of Stratospheric Ozone, Volume 74*, International Geophysics Series, (Academic Press, San Diego)
- Douglass, A. R., Jackman, C. H., & Stolarski, R. S. 1989, *J. Geophys. Res.*, 94, 9862
- Ellis, J., & Schramm, D. N. 1995, *Proc. Natl. Acad. Sci. USA*, 92, 235
- Fleming, E. L., Jackman, C. H., Stolarski, R. S., & Considine, D. B. 1999, *J. Geophys. Res.*, 104, 23911
- Fleming, E. L., Jackman, C. H., Considine, D. B., & Stolarski, R. S. 2001, *J. Geophys. Res.*, 106, 14245

- Gehrels, N., Leventhal, M., MacCallum, C. J., 1988, in Nuclear Spectroscopy of Astrophysical Sources, AIP Conf. 170, eds. N. Gehrels, G. Share (AIP, New York), 87
- Jackman, C. H., Douglass, A. R., Rood, R. B., & McPeters, R. D. 1990, *J. Geophys. Res.*, 95, 7417
- Jackman, C. H., Fleming, E. L., Chandra, S., Considine, D. B., & Rosenfield, J. E. 1996, *J. Geophys. Res.*, 101, 28753
- Jackman, C. H., Fleming, E. L., & Vitt, F. M. 2000, *J. Geophys. Res.*, 105, 11659
- Laster, H. 1968, *Science*, 160, 1138
- Madronich, S., McKenzie, R. L., Bjorn, L. O., Caldwell, M. M. 1998, *J. Photochem. and Photobiol. B Biology*, 46, 5
- Maiz-Apellaniz, J. 2001, *AJ*, 121, 2737
- Muller, R., & Crutzen, P. J. 1993, *J. Geophys. Res.*, 98, 20483
- Neher, H. V. 1961, *J. Geophys. Res.*, 66, 4007
- Neher, H. V. 1967, *J. Geophys. Res.*, 72, 1527
- Neher, H. V. 1971, *J. Geophys. Res.*, 76, 1637
- Nicolet, M. 1975, *Planet. Space Sci.*, 23, 637
- Plechaty, E. F., Cullen, D. E., & Howerton, R. J. 1981, *Tables and Graphs of Photon-Interaction Cross Sections From 0.1 keV to 100 MeV Derived From the LLL Evaluated Nuclear-Data Library Tables and Graphs of Photon-Interaction Cross* (Lawrence Livermore Laboratory; Berkeley)
- Porter, H. S., Jackman, C. H., & Green, A. E. S. 1976, *J. Chem. Phys.*, 65, 154
- Reid, G. C., McAfee, J. R., & Crutzen, P. J. 1978, *Nature*, 275, 489

Ruderman, M. A. 1974, *Science*, 184, 1079

van den Bergh, S. 1994, *PASP*, 106, 689

Vitt, F. M., & Jackman, C. H. 1996, *J. Geophys. Res.*, 101, 6729

Weaver, T. A., & Woosley, S. E. 1993, *Phys. Rep.*, 227, 65

Webber, W. R. 1998, *ApJ*, 506, 329

Whitten, R. C., Cuzzi, J., Borucki, W. J., & Wolfe, J. H. 1976, *Nature*, 263, 398

FIGURE CAPTIONS

Figure 1. Contour plot of global average of ozone depletion during Year 2 from gamma irradiation, for $D_{\text{SN}} = 10$ pc and $i_{\text{SN}} = 0^\circ$.

Figure 2. Contour plot of global average of ozone depletion during Year 20 due to the cosmic irradiation, assuming an enhancement of 100-fold in the empirically observed GCR ionization rate, and $i_{\text{SN}} = 0^\circ$.

Figure 3. Peak annual average reduction in global ozone from gamma irradiation for $D_{\text{SN}} = 10$ pc as a function of i_{SN} (average over Year 2).

Figure 4. Annual average reduction in global ozone from gamma irradiation from a SN as a function of D_{SN} , assuming $i_{\text{SN}} = 0^\circ$ (average over Year 2). The solid line indicates a dependency of D_{SN}^{-2} .

This figure "Figure1.jpg" is available in "jpg" format from:

<http://arxiv.org/ps/astro-ph/0211361v1>

This figure "Figure2.jpg" is available in "jpg" format from:

<http://arxiv.org/ps/astro-ph/0211361v1>

